Cone penetration test-based correlations to forecast critical state parameters

Joseph Gamez[1#] and *Scott* Olson[2]

[1]*Engineer Research and Development Center, Construction Engineering Research Laboratory, 2902 Newmark Drive, Champaign, IL, USA*
[2]*University of Illinois at Urbana-Champaign, Department of Civil and Environmental Engineering, 205 N. Mathews Avenue, Urbana, IL, USA*
[#]*Corresponding author: joseph.a.gamez@usace.army.mil*

ABSTRACT

In critical state soil mechanics, the critical state refers to the combination of effective stress and void ratio (e) at which a soil continues to shear with no change in effective stress, shear stress, and e. The phenomena can be visualized using the critical state line (CSL). The CSL represents the locus of e at critical state with effective mean stress (σ'_{mean}). To define the CSL, the CSL slope (λ), termed "compressibility," and CSL y-axis intercept at 1 kPa (Γ), termed "altitude," are required. The CSL in $e - \sigma'_{mean}$ space provides a simple model of complex soil behavior that allows engineers to construct constitutive models using the state parameter (ψ), which is the mathematical difference between the in-situ e of the soil and the e of the soil at critical state. Currently, Γ can be obtained only through laboratory testing, while λ and ψ can be obtained via laboratory testing or correlation. This paper presents forthcoming correlations based on the Δ_Q soil behavior index (which is obtained via the cone penetration test, CPT) to forecast Γ, λ, and ψ, and compares the Δ_Q-based correlations' performance to other CPT-based correlations as well as to data obtained from literature. To compare the correlations, the authors used data from a site investigation performed in Fraser River sand as part of the Canadian Liquefaction Experiment.

Keywords: cone penetration test; altitude; compressibility; state parameter.

1. Introduction

The Canadian Liquefaction Experiment (CANLEX) was a collaborative research program performed from 1993 to 1997 that combined the efforts of nearly twenty organizations from government, industry, and academia. As the behavior of loose sandy soils can be difficult to forecast and can also have major financial consequences, CANLEX aimed to (1) develop test sites to study sand characterization, (2) develop and evaluate undisturbed sampling techniques, (3) calibrate and evaluate in-situ testing techniques, and (4) obtain an improved understanding of the phenomenon of soil liquefaction (Wride and Robertson 1997). To accomplish these goals, CANLEX researchers performed in-situ testing in tandem with drilling, boring, sampling, and laboratory testing. These activities produced significant amounts of data for six CANLEX project sites, including the Massey site, which is the focus of this study.

Using data from the Massey site, the authors compare recently developed correlations for the cone penetration test (CPT) using the Δ_Q soil behavior index. This study builds on work by Ghafghazi and Shuttle (2008) and Ghafghazi (2011), wherein correlations to forecast state parameter were compared to laboratory data. While Ghafghazi (2011) used correlations from Been et al. (1987), Plewes et al. (1992), Konrad (1997), and Ghafghazi and Shuttle (2008) and Ghafghazi (2011), the authors note that the correlation by Konrad (1997) was removed since it could be used only at discrete depths (rather than continuously), the Been et al. (1987) correlation was updated to a similar correlation from Jefferies and Been (2016), and a correlation from Robertson (2009, 2012) was added. The authors also compare a Δ_Q-based correlation for the slope of the critical state line to correlations by Been and Jefferies (1992) and Plewes et al. (1992) and to laboratory data, as well as a correlation for the y-axis intercept of the critical state line at 1 kPa to laboratory data.

2. The Critical State Line

In critical state soil mechanics, the critical state refers to the combination of effective stress and void ratio (e) at which a soil continues to shear with no change in effective stress, shear stress, and e. The phenomena can be visualized using the critical state line (CSL), as illustrated in Figure 1. The CSL represents the locus of e at critical state with effective mean stress (σ'_{mean}). To define the CSL, the CSL slope (λ), termed "compressibility," and CSL y-axis intercept at 1 kPa (Γ), termed "altitude," are required. The CSL in $e - \sigma'_{mean}$ space provides a simple model of complex soil behavior that allows engineers to construct constitutive models for detailed analyses using the state parameter (ψ), which is the mathematical difference between the in-situ e of the soil and the e of the soil at critical state.

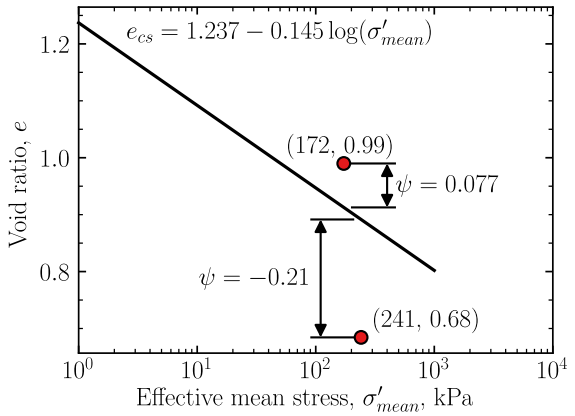

Figure 1. Example of the CSL from Chattahoochee sand (after Gamez and Olson [Forthcoming]). Two tests from Al-Awkati (1975) are plotted to illustrate ψ.

3. The Δ_Q Soil Behavior Index

Saye et al. (2017) introduced the Δ_Q soil behavior index, which describes a linear relationship between effective stress-normalized cone tip resistance, $Q_t = (q_t - \sigma_v) / \sigma'_v$, and effective stress-normalized friction sleeve resistance, f_s / σ'_v; where q_t = cone tip resistance corrected for unequal end area effects, σ_v = total vertical stress, σ'_v = effective vertical stress, and f_s = friction sleeve resistance. The Δ_Q index is the slope of the line created when Q_t is plotted against f_s / σ'_v (Figure 2) and is given by the equation:

$$\Delta_Q = \frac{Q_t + 10}{f_s/\sigma'_v + 0.67} \quad (1)$$

The Δ_Q soil index applies to soils ranging from sands to clays and peats, but like all soil behavior indices, has limited applicability to structured and highly sensitive soils. It should also be noted that Δ_Q is relatively unaffected by overconsolidation (i.e., Δ_Q remains relatively constant in a soil mass composed of a homogenous soil type that has normally consolidated and overconsolidated layers).

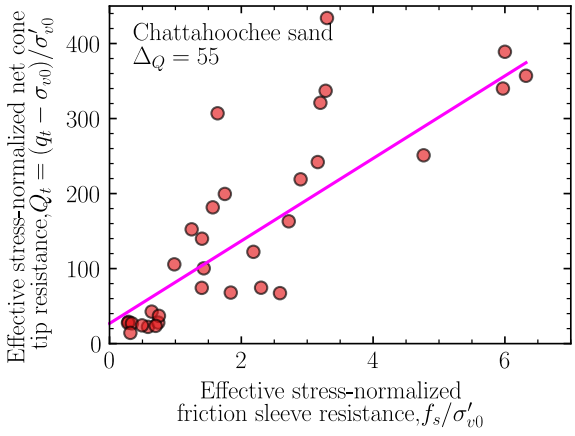

Figure 2. Example of the interpretation of Δ_Q for Chattahoochee sand from CPTs performed in a calibration chamber (after Gamez and Olson [Forthcoming]).

Saye et al. (2017) presented correlations between Δ_Q and soil behavior type as well as several other soil index properties, such as fines content, median particle diameter, liquid limit, and plasticity index. Gamez and Olson (Forthcoming) developed further correlations, (some of which were previously mentioned) to forecast (1) Γ, (2) λ, (3) ψ, and (4) relative density, while Gamez and Olson (Forthcoming) developed a Δ_Q-based overburden normalization.

4. Location

The Massey site is located outside of Vancouver, British Columbia on Deas Island. The site is located at the south end of the Massey Tunnel, which connects Richmond and Delta, and on the southern shore of the Fraser River (Monahan et al. 1994; Wride and Robertson 1997; Ghafghazi 2011). The site consists of deltaic deposits, which Monahan et al. (1994) and Wride and Robertson (1997) describe as naturally deposited sands approximately 200 years in age. The water table at the site sits at an average depth of 2.3 m (Ghafghazi 2011).

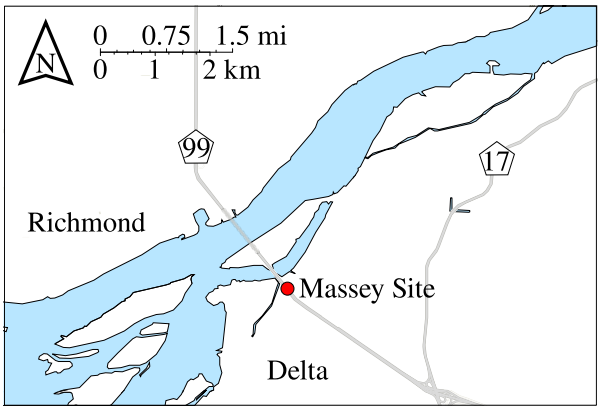

Figure 3. The Massey Site is located south of Vancouver, and connects Richmond and Delta (after Wride and Robertson 1997).

Site characterization at the Massey site targeted a zone from 8 – 13 m in depth. In the targeted zone, CANLEX researchers performed CPTs, standard penetration tests, shear wave velocity measurements, pressuremeter tests, and geophysical logging. Researchers accompanied in-situ testing with soil sampling via ground freezing and the Laval Large Diameter Sampler (LDS). The in-situ testing and LDS sampling were performed concentrically around the ground freezing location at distances of approximately 5 m (Figure 4). The cone traces from CPTs M4901 – M4906 over the targeted 5-m-thick depth range are presented in Figure 5.

4.1. Fraser River Sand

Fraser River sand is a uniform sand with angular to subangular grains with low to medium sphericity (Ghafghazi 2011). CANLEX researchers characterized certain index properties of three samples of sand: the University of British Columbia (UBC) sample (Shozen 2001), the Massey (M) sample (Ghafghazi 2011), and the University of Alberta (U of A) sample (Chillarige 1995). The maximum void ratio (e_{max}), minimum void ratio (e_{min}), and specific gravity (G_s) of each sample were found to be similar: $0.989 \leq e_{max} \leq 1.056$, $0.600 \leq e_{min} \leq$

0.627, and 2.68 ≤ G_s ≤ 2.75. Chillarige (1995) and Ghafghazi (2011) also characterized Γ and λ of the Fraser River sand samples, though ranges for these parameters were large: 1.11 ≤ Γ ≤ 1.22 and 0.067 ≤ λ_{10} ≤ 0.14. The index properties and critical state parameters for the UBC, Massey, and U of A samples are summarized in Table 1.

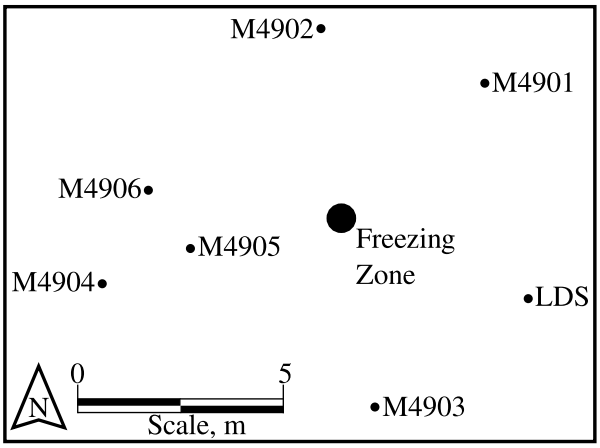

Figure 4. Plan view showing the in-situ testing and sampling locations at the Massey Site (after Wride and Robertson 1997).

Table 1. Index properties and critical state parameters of Fraser River sand as determined by three laboratories.

	Sample		
	UBC	Massey	U of A
e_{max}	0.989	1.056	1.00
e_{min}	0.627	0.677	0.600
G_s	2.72	2.68	2.75
Γ	1.22	1.17	1.11
λ_{10} (λ_e)	0.14 (0.060)	0.081(0.035)	0.067 (0.029)

4.2. Comparison of Correlations

The authors extend the work by Ghafghazi (2011) and compare five ψ correlations, including a Δ_Q-based correlation, against field data from the Massey site. Additionally, the authors compare a Δ_Q-based correlation for Γ against laboratory data as well as a Δ_Q-based correlation for λ_{10} against two other correlations and laboratory data. In keeping with Ghafghazi (2011), the authors: (1) used the upper and lower bounds of the CPT data (Figure 5) to define the input data for the correlations and (2) excluded portions of CPT data from approximately 12 – 13 m from CPTs M4901 and M4902 since, as Ghafghazi (2011) suggests, there is a "discrepancy with the trend established by the rest of the tests" (Figure 5).

4.2.1. Δ_Q correlations

Gamez and Olson (Forthcoming) and Gamez (Forthcoming) developed Δ_Q-based correlations to forecast Γ, λ_{10}, and ψ. The Δ_Q-based correlations were developed using a database of 847 CPTs performed in sand-filled calibration chambers involving 31 studies, 17 calibration chambers, and 24 sandy soils. The Δ_Q-based correlations for Γ, λ_{10}, and ψ are given by the equations:

$$\Gamma = \frac{1.47}{e^{(0.018\Delta_Q)}} + 0.70 \quad (2)$$

$$\lambda_{10} = \frac{0.72}{e^{(0.032\Delta_Q)}} + 0.020 \quad (3)$$

$$\psi = a\log(\Delta_Q) + b \quad (4)$$

Coefficients a and b can be computed using the equations:

$$a = 0.12\log(Q_t) \quad (5)$$

$$b = 0.52 - 0.42\log(Q_t) \quad (6)$$

The authors note that Eqns. (2), (3), and (4) are valid over a range of 25 ≤ Δ_Q ≤ 210; while Eqns. (5) and (6) are valid over a range of 1 ≤ Q_t ≤ 500.

4.2.2. Methodology

The $\Delta_Q - \Gamma$ correlation is compared only to laboratory data since, to the authors' knowledge, no other CPT-based Γ correlations are available in the literature. The $\Delta_Q - \lambda$ correlation is compared to Been and Jefferies (1992) and Plewes et al. (1992) as well as to laboratory data. The authors also compared the $\Delta_Q - \psi$ correlation against correlations from Plewes et al. (1992), Ghafghazi (2011), Robertson (2012), and Jefferies and Been (2016). Though the length of this article prohibits a detailed discussion on each correlation, the parameters used in their calculations are presented in Table 2. In keeping with Ghafghazi (2011), the authors used the critical state parameters from the Massey sample to estimate the field values of ψ.

5. Results and Discussion

The authors calculated the $\Delta_Q - \Gamma$, $\Delta_Q - \lambda_{10}$, and $\Delta_Q - \psi$ correlations by first calculating Δ_Q for upper and lower bound CPT traces (Figure 6) using Eqns. (2), (3), and (4). As illustrated in Figure 6, from depths between approximately 8 – 11 m, the $\Delta_Q - \Gamma$ correlation forecasts lower values of Γ than the UBC and Massey data, though the upper bound forecast of Γ is in line with the U of A data. Between approximately 11 – 12 m, the $\Delta_Q - \Gamma$ correlation generally forecasts Γ between the Massey and U of A data. At depths of approximately 12 – 13 m, the $\Delta_Q - \Gamma$ correlation forecasts Γ directly in line with the three laboratory values of Γ, where the lower bound forecast is in line with Γ_{UA}, the upper bound forecast is in line with Γ_{UBC}, and the average is approximately in line with Γ_M.

With regard to the λ_{10} forecasts (Figure 6), both the Been and Jefferies (1992) and Plewes et al. (1992) correlations forecast lower than the laboratory values for the entire target zone depth range. From depths between 8 – 11 m, the lower bound of the $\Delta_Q - \lambda_{10}$ forecast is approximately in line with $[\lambda_{10}]_{UA}$ while the average value is approximately in line with $[\lambda_{10}]_M$. From 11 – 12 m, the lower bound $\Delta_Q - \lambda_{10}$ forecast is approximately in line with $[\lambda_{10}]_M$, and from 12 – 13 m, the lower bound of the $\Delta_Q - \lambda_{10}$ forecast is in line with $[\lambda_{10}]_M$ and the upper bound is in line with $[\lambda_{10}]_{UBC}$.

The laboratory values of ψ exhibit a wide range and are scattered throughout the target zone depth range (Figure 7). Additionally, using different values of λ_{10} (i.e., $[\lambda_{10}]_{UBC}$ or $[\lambda_{10}]_{UA}$) would shift the laboratory values of ψ such that certain correlations would appear to forecast better than others. Thus, the authors mainly

focus the comparison of the ψ correlations to their performance relative to each other rather than to the laboratory data.

In general, the Jefferies and Been (2016) correlation forecasts ψ denser than the other correlations, while the Ghafghazi (2011) and Robertson (2012) correlations forecast looser than others. The Plewes et al. (1992) correlation tended to forecast ψ in approximately the median of all the correlations; however, this correlation exhibited the widest range of forecasted ψ, especially between 8 – 8.5 m. The $\Delta_Q - \psi$ correlation also forecast near the median of all correlations, with its lower bound forecast similar to that of the lower bound of the Plewes et al. (1992) correlation and its upper bound forecast similar to the lower bound of the Robertson (2012) correlation. While the laboratory data does not provide conclusive insight on the performance of each ψ correlation, each correlation's forecast is within the range of the laboratory data. With regard to the scatter in the laboratory data, Ghafghazi (2011) and Ghafghazi and Shuttle (2010) noted that the scatter was more likely caused by the ground sampling techniques rather than e variations in situ.

The results from this study indicate that several correlations not only forecast ψ looser or denser compared to others, but also forecast values similar to others. In particular, the Jefferies and Been (2016) correlation forecast the densest conditions, while the Ghafghazi (2011) and Robertson (2012) correlations forecast the loosest. The Ghafghazi (2011) and Robertson (2012) correlations also forecast similar values of ψ, but the Robertson (2012) correlation has the benefit of being simpler to calculate. The Plewes et al. (1992) correlation and $\Delta_Q - \psi$ correlation forecast in the median range of the correlations. While both correlations are simple to compute, the Plewes et al. (1992) correlation exhibited more variability. Thus, the authors suggest that certain correlations may forecast upper and lower bounds of ψ. As an initial screening tool, for example, engineers could use the Robertson (2012) correlation as an upper bound and the $\Delta_Q - \psi$ correlation as a median or lower bound. (Note that while the Jefferies and Been [2016] correlation forecasted lower ψ, it requires laboratory data.)

6. Conclusions

This paper compares CPT-based correlations for Γ, λ_{10}, and ψ to similar correlations from the literature and to laboratory data. Based on the work performed in this study, the authors conclude the following.

1. The $\Delta_Q - \Gamma$ correlation reasonably forecasts within the range of laboratory data at the Massey Site. The authors note, however, the $\Delta_Q - \Gamma$ correlation generally forecast lower than the measured values from depths of 8 – 10.5 m (the target zone was from depths of 8 – 13 m).
2. The $\Delta_Q - \lambda_{10}$ correlation reasonably forecasts within the range of laboratory data at the Massey Site. Indeed, upper and lower bound forecasts of λ_{10} were bounded by three laboratory values of λ_{10}, where the lower values of the $\Delta_Q - \lambda_{10}$ forecast approximately equaled $[\lambda_{10}]_{UA}$, upper bound values approximately equaled $[\lambda_{10}]_{UBC}$, and average values approximately equaled $[\lambda_{10}]_M$.
3. While the authors could not conclusively compare the ψ correlations to the laboratory data, the analysis indicated that some correlations tend to forecast denser conditions than others while others tend to forecast looser conditions. The analysis also indicated that certain correlations forecast values of ψ similar to each other. Considering this, the authors suggest that, as an initial screening tool, the Robertson (2012) correlation may be used as an upper bound forecast and that the $\Delta_Q - \psi$ correlation may be used as a median or lower bound forecast (since the Jefferies and Been [2016] correlation forecasted the lowest values of ψ, but requires laboratory data).

Data Availability

The authors digitized the data used in this study with free and open source software developed by Rohatgi (2022). The digitized data as well as the calculations can be found in open-source format at: https://doi.org/10.17603/ds2-v5sp-3g45.

Table 2. Parameters used to compute each correlation.

Correlation	λ_{10}	M^*	$G_{max}{}^\dagger$	$I_c{}^\ddagger$ (the variable $B_q{}^\S$ is defined below)
Gamez and Olson (Forthcoming)	$\frac{0.72}{e^{(0.032\Delta_Q)}} + 0.020$	-	-	-
Plewes et al. (1992)	$\frac{F_r}{10}$	1.20	-	-
Been and Jefferies (1992)	$\frac{1}{34 - 10I_c}$	-	-	$\sqrt{\{3 - \log[Q_t(1 - B_q) + 1]\}^2 + \{1.5 + 1.3(\log F_r)\}^2}$
Ghafghazi (2011)	0.081	-	Figure 5d	-
Jefferies and Been (2016)	0.081	1.49	-	$\sqrt{\{3 - \log[Q_t(1 - B_q) + 1]\}^2 + \{1.5 + 1.3(\log F_r)\}^2}$
Robertson (2012)	-	-	-	$\sqrt{(3.47 - \log[Q_t])^2 + (1.22 + \log[F_r]^2)}$

*M = critical state friction angle
‡G_{max} = shear modulus
‡I_c = soil behavior index
§B_q = normalized excess pore pressure = $(u - u_0) / (q_t - \sigma_{v0})$; where u = penetration induced pore pressure and u_0 = hydrostatic pore pressure

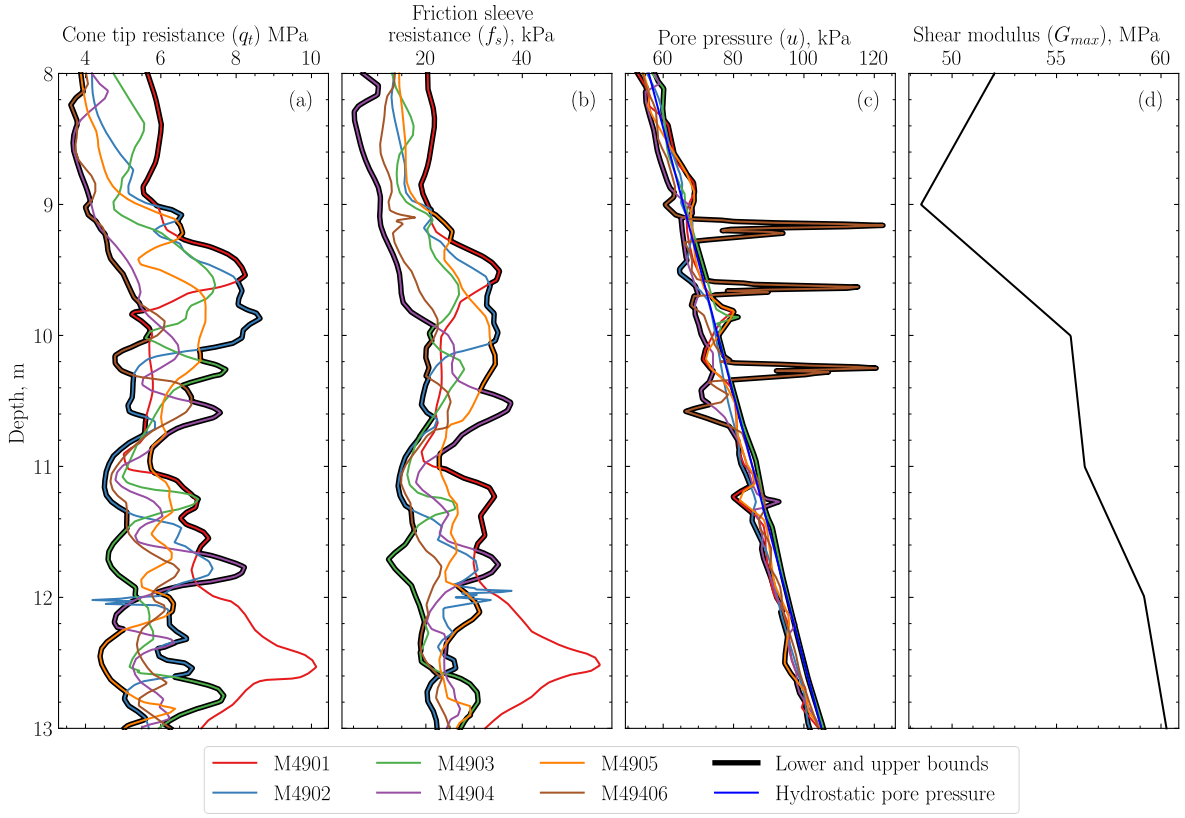

Figure 5. Plots of (a) q_t, (b) f_s, (c) u_2, and (d) G_{max} from the Massey site characterization (after Ghafghazi 2011). In keeping with Ghafghazi (2011), the upper and lower bound traces were created (but exclude portions of data from CPTs M4901 and M4902) and were used with each correlation to compute soil parameters presented in this study.

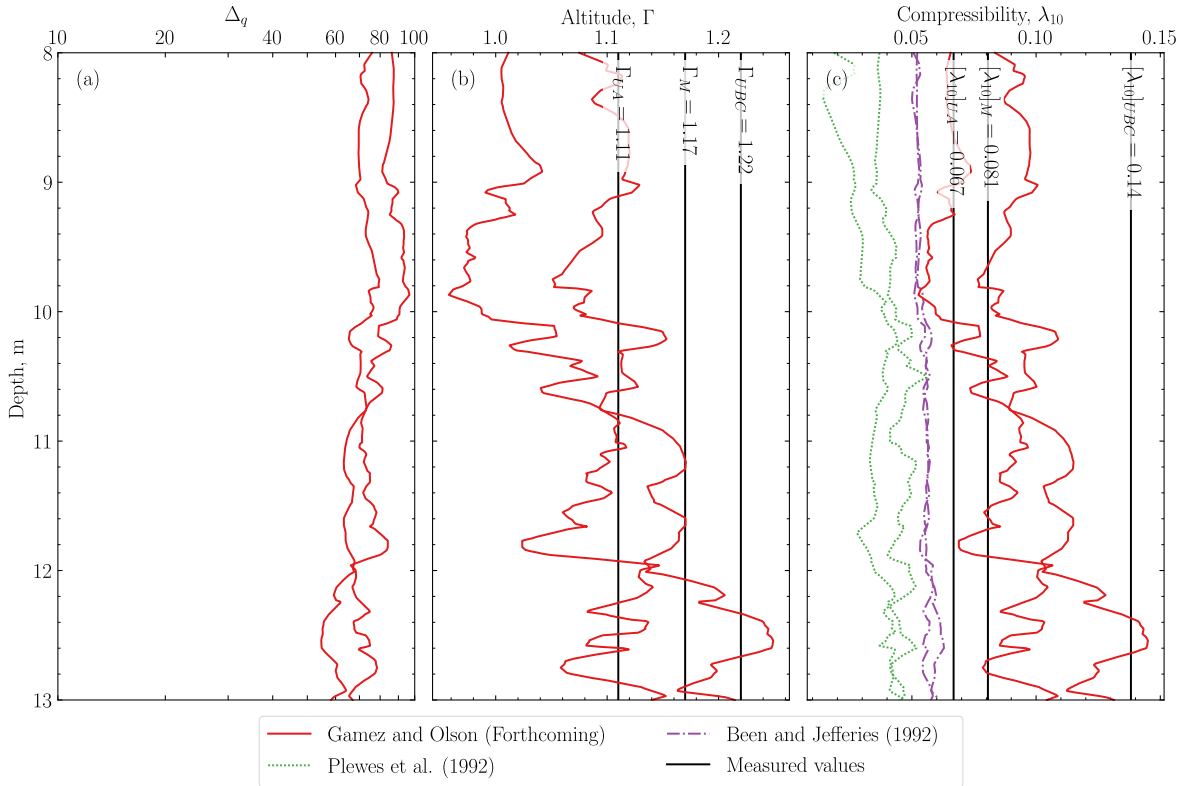

Figure 6. Plots of (a) Δ_Q – depth, (b) Γ – depth (using Eqn. [2]), and (c) λ_{10} – depth (using Eqn. [3]). Plot (b) also shows the performance of the $\Delta_Q - \Gamma$ correlation compared to laboratory data, and plot (c) includes the performance of correlations by Been and Jefferies (1992) and Plewes et al. (1992).

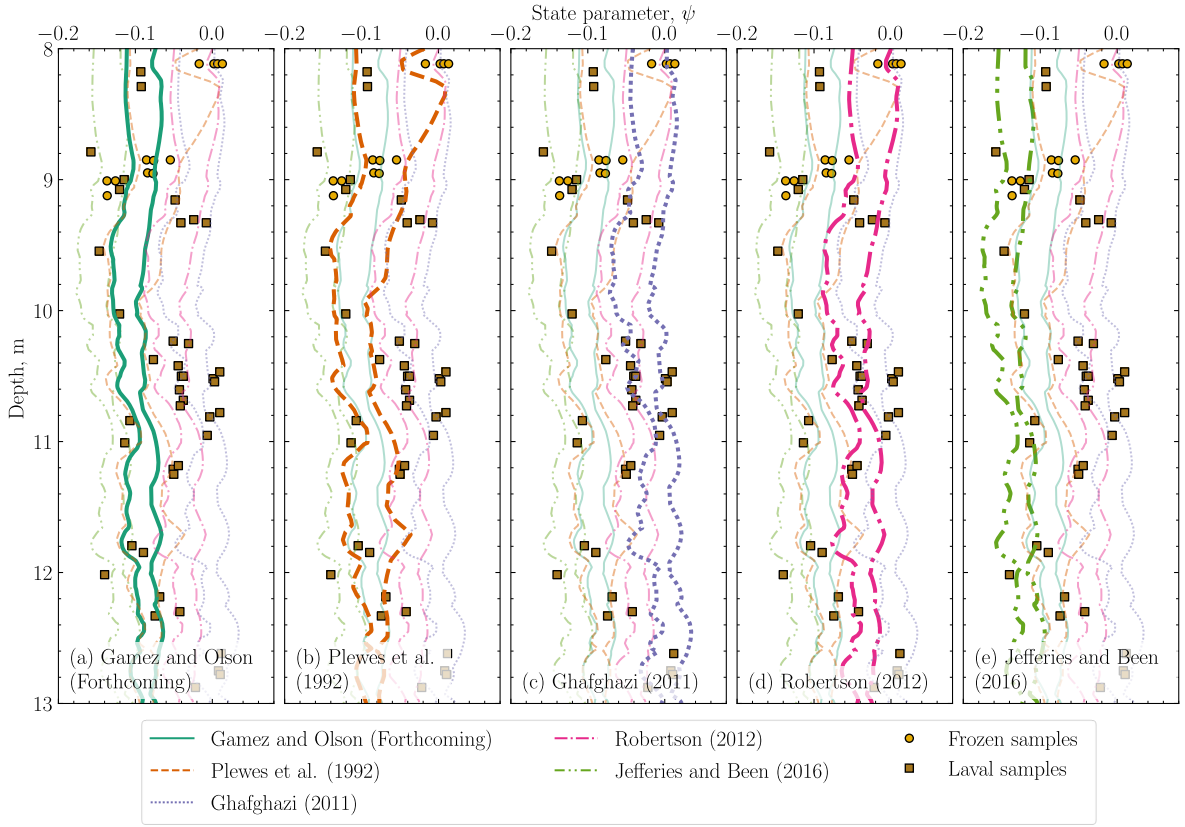

Figure 7. Comparison of the ψ correlations versus depth: (a) Gamez and Olson (Forthcoming), (b) Plewes et al. (1992), (c) Ghafghazi (2011), (d) Robertson (2012), and (e) Jefferies and Been (2016).

References

Al-Awkati, Z. A. 1975. "On problems of soil bearing capacity at depth." Ph. D. thesis. Durham, NC: Duke University.

Been, K., and M. G. Jefferies. 1992. "Towards systematic CPT interpretation." *Predict. Soil Mech.*, 121–134. Oxford, England: Thomas Telford Publishing.

Been, K., M. G. Jefferies, J. H. A. Crooks, and L. Rothenburg. 1987. "The cone penetration test in sands: part II, general inference of state." *Géotechnique*, 37 (3): 285–299.

Chillarige, A. V. 1995. "Liquefaction and seabed instability in the Fraser River Delta." Ph. D. Edmonton, Canada: University of Alberta.

Gamez, J. A. Forthcoming. "Compressibility-based interpretation of cone penetration test data." Ph. D. Urbana, IL: University of Illinois.

Gamez, J. A., and S. M. Olson. Forthcoming. "In-Situ interpretation of critical state parameters and relative density using the cone penetration test." *Forthcoming*.

Gamez, J. A., and S. M. Olson. Forthcoming. "Compressibility-based correlations for sandy soils to forecast cone tip resistance and effective overburden normalization." *Forthcoming*.

Ghafghazi, M. 2011. "Towards comprehensive interpretation of the state parameter from cone penetration testing in cohesionless soils." PhD Thesis. Vancouver, Canada: University of British Columbia.

Ghafghazi, M., and D. Shuttle. 2008. "Interpretation of sand state from cone penetration resistance." *Géotechnique*, 58 (8): 623–634.

Ghafghazi, M., and D. A. Shuttle. 2010. "Interpretation of the in situ density from seismic CPT in Fraser River sand." *2nd Int. Sympoisum Cone Penetration Test.* Huntington Beach, CA.

Jefferies, M., and K. Been. 2016. *Soil liquefaction: a critical state approach*. Boca Raton, FL: CRC press.

Konrad, J.-M. 1997. "In situ sand state from CPT: evaluation of a unified approach at two CANLEX sites." *Can. Geotech. J.*, 34 (1): 120–130. NRC Research Press Ottawa, Canada.

Monahan, P. A., J. L. Luternauer, and J. V. Barrie. 1994. "The geology of the CANLEX Phase II sites in Delta and Richmond British Columbia." *Proc 48th Can. Geotech. Conf.*, 59–68. Vancouver, Canada: Canadian Geotechnical Society.

Plewes, H. D., M. P. Davies, and M. G. Jefferies. 1992. "CPT based screening procedure for evaluating liquefaction susceptibility." *Proc 45th Can Geotech Conf*, 1–9. Toronto, Ontario.

Robertson, P. K. 2009. "Interpretation of cone penetration tests—a unified approach." *Can Geotech J*, 46 (11): 1337–1355. NRC Research Press.

Robertson, P. K. 2012. "The James K. Mitchell Lecture: Interpretation of in-situ tests–some insights." *Proc 4th Int Conf Geotech. Geophys. Site Charact.*, 3–24. Porto de Balinhas, Brazil: Taylor & Francis Group.

Rohatgi, A. 2022. *WebPlotDigitizer*. https://automeris.io/WebPlotDigitizer.

Saye, S. R., J. Santos, S. M. Olson, and R. D. Leigh. 2017. "Linear trendlines to assess soil classification from cone penetration test data." *J Geotech Geoenv Eng*, 143 (9): 04017060.

Shozen, T. 2001. "Deformation under the constant stress state and its effect on stress-strain behaviour of Fraser River Sand." PhD Thesis. Vancouver, Canada: University of British Columbia.

Wride, C. E., and P. K. Robertson. 1997. *Phase II Data Review Report (Massey and Kidd sites, Fraser River Delta)*. Technical Report. Edmonton, Canada: University of Alberta.